Engineering Science and Technology, an International Journal 19 (2016) 1985–1992

HOSTED BY

ELSEVIER

Contents lists available at ScienceDirect

Engineering Science and Technology, an International Journal

journal homepage: www.elsevier.com/locate/jestch

Full Length Article

Variable viscosity and MHD flow in Casson fluid with Cattaneo–Christov heat flux model: Using Keller box method

M.Y. Malik, Mair Khan, T. Salahuddin *, Imad Khan

Department of Mathematics, Quaid-i-Azam University, Islamabad 44000, Pakistan

ARTICLE INFO

Article history:
Received 23 February 2016
Revised 24 May 2016
Accepted 22 June 2016
Available online 16 July 2016

Keywords:
Variable viscosity
Cattaneo–Christov heat flux model
Stretching sheet with variable thickness
MHD flow
Casson fluid
Keller box method

ABSTRACT

This article presents a numerical investigation of MHD flow of Casson fluid model with variable viscosity towards a stretching sheet with variable thickness. Cattaneo–Christov heat flux model is used instead of Fourier's law to explore the heat transfer characteristics. The governing partial differential equations are transformed into nonlinear ordinary differential equations by using suitable similarity transformations. These equations are solved by using a numerical technique, known as Keller box method. The relevant physical parameters appearing in velocity and temperature distributions are analyzed and discussed through graphs. In order to check the accuracy of the method comparison has been made with some previous published results.

1. Introduction

The study of non-Newtonian fluids is an important topic for researchers due its industrial applications in construction of paper production, polymer sheet, hot rolling, glass-fabric, wire drawing and petroleum production. The tangent hyperbolic fluid, Maxwell fluid, Williamson fluid, viscoelastic fluids, etc. are non-Newtonian fluids describing the nonlinearity behavior. Casson fluid model is one of the most commonly used rheological model and has number of examples such as blood, fruit juices, soup, sauce, chocolate, etc. Nadeem et al. [1] studied the boundary layer flow of a Casson fluid for a heat transfer towards an exponentially stretching surface in presence of thermal radiation. Mukhopadhyay et al. [2] presented the concept of two-dimensional flow over unsteady stretching surface. Mukhopadyay [3] discussed the boundary layer for a Casson fluid and heat transfer passing through a nonlinear stretching surface. Nadeem et al. [4] investigated three-dimensional steady flow of Casson fluid past a porous linear stretching sheet. Mukhopadhyay et al. [5] investigated the numerical solution for a steady boundary layer flow and heat transfer in a Casson fluid over exponentially stretching permeable surface with prescribed heat flux. Mahanta et al. [6] presented the concept of MHD three-dimensional Casson fluid pass a porous linear stretching sheet. Mustafa et al. [7] studied the boundary layer flow for a Casson nano fluid convinced by nonlinear stretching surface. Animasaun et al. [8] investigated the boundary layer flow for steady incompressible laminar free convective magneto-hydrodynamic (MHD) Casson fluid over an exponential stretching surface rooted in a thermal stratified medium. Das et al. [9] analyzed the effect of mass and heat transfer for unsteady Casson fluid in a vertical plat. Raju et al. [10] discussed the heat and mass transfer of Casson fluid over an exponentially porous stretching sheet. Ramesh et al. [11] presented the idea of generalized Couette flow for an incompressible Casson fluid between the same plates using same boundary condition. Khalid et al. [12] investigated the free convection flow of a Casson fluid over a fluctuating vertical plat with constant wall temperature.

The study of boundary layer flow over a continuously stretching sheet has practical applications in physics, chemistry and engineering. Many metallurgical processes such as drawing of plastic films, annealing, thinning of copper wires, etc plays an important role for governing momentum and heat transfer boundary layer flow for a stretching sheet. Ganesh et al. [13] investigated the numerical solution for nano-fluid over linearly semi-infinite stretching sheet in the presence of magnetic field. Dessie et al. [14] presented the concept of MHD flow for incompressible viscous fluid and heat transfer phenomena over a stretching sheet embedded in porous medium in presence of heat source/sink and viscous dissipation. Hakeem et al. [15] studied the effect of partial slip on hydro-magnetic boundary layer flow and heat transfer due to stretching surface with thermal radiation. Ene et al. [16]

* Corresponding author.

Peer review under responsibility of Karabuk University.

http://dx.doi.org/10.1016/j.jestch.2016.06.008
2215-0986/

investigated the approximate solution for steady boundary layer flow and heat transfer over an exponentially stretching sheet. Abass et al. [17] presented the laminar flow for a viscous fluid due to unsteady stretching/shrinking cylinder with partial slip conditions. Hayat et al. [18] investigated the hydromagnetic third-grade fluid over a continuously stretching cylinder and solved the problem via homotopic procedure. Malik et al. [19] studied the approximate solution for MHD flow of tangent hyperbolic fluid model over a stretching cylinder. Sandeep et al. [20] deliberated the concept of two dimensional MHD radiative flows and heat transfer of a dusty nano fluid over exponentially stretching surface.

The study of non-flatness stretching sheet with variable thickness is useful in the mechanical, civil, marine, aeronautical structure and designs. Fang et al. [21] investigated numerically the boundary layer flow of viscous fluid over a stretching sheet with variable thickness. Khader et al. [22] studied two dimensional boundary layer flows over a continuously stretching sheet with variable thickness by encountering the slip. Sarangi et al. [23] analyzed the boundary layer flow and heat transfer of two dimensional two phase flow over a stretching sheet. Khader et al. [24] investigated the boundary layer flow for a Newtonian fluid over a permeable stretching sheet with power law surface over a stretching sheet with variable thickness. Hayat et al. [25] studied the boundary layer flow for a Maxwell fluid over a stretching sheet with variable thickness.

The classical Fourier's law describes the heat transfer mechanism for relevant situations. The major drawback for parabolic energy equation is that unique disturbance is felt instantly throughout whole medium. Cattaneo–Cheristov heat flux model is the modified Fourier's form which gives thermal relaxation time. Christov [26] amended the Cattaneo's law by thermal relaxation time along with Oldroyd's upper-convicted derivative, in order to preserve the material invariance of the model. Han et al. [27] presented the coupled flow and heat transfer in viscoelastic fluid over a stretching plat with velocity slip boundary. Raju et al. [28] studied the numerically solution for heat and mass transfer behavior of Casson fluid over an exponentially stretching sheet. Mustafa [29] investigated the Cattaneo–Christov heat flux model in a rotating flow of viscoelastic fluid bounded by stretching surface.

From published literature it is observed that steady MHD flow of Casson fluid over a stretching sheet with variable thickness has not been discussed so far. The viscosity of the fluid is assumed to be erratic with temperature. Cattaneo–Christov heat flux model which is a modified version of the classical Fourier's law is used in this work to explore the insight of heat transfer phenomena. For better accuracy the modeled differential equations are solved numerically using Keller box method. The behavior of different pertinent parameters on velocity and temperature profiles is discussed in detail.

2. Mathematical formulation

Consider the steady two-dimensional incompressible boundary layer flow of Casson fluid over stretching sheet with variable thickness. The velocity of sheet is assumed to be $U_w = U_0(x+b)^m$, where U_0 the reference velocity is. It is assumed that the wall thickness of the stretching sheet may increase or decrease with distance from slot by varying the power index m.

For $m = 1$ the problem reduces to flat stretching sheet. The viscosity of the fluid is assumed to be variable i.e., $\mu = \mu_0 e^{\varepsilon(T-T_\infty)}$. Cattaneo–Christov heat flux model is used instead of Fourier' s law to explore the heat transfer characteristic. Cartesian coordinates x-axis along the sheet with y-axis are taken normal to it. The magnetic field of strength B_0 is applied normal to the sheet (as shown in Fig. 1).

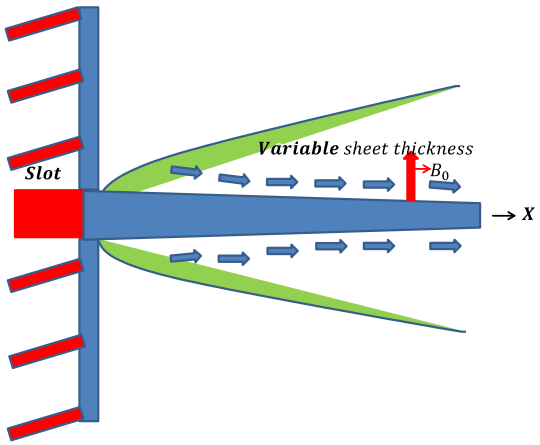

Fig. 1. Stretching sheet with variable.

$$\nabla.V = 0, \tag{1}$$

$$\rho\frac{DV}{Dt} = \nabla.\tau + \rho b, \tag{2}$$

where V is the velocity field, ρ is the density, $\frac{D}{Dt}$ material time derivative, τ is Cauchy stress tensor, ∇ operator and $b = J \times B\rho$ is the body force. The stress tensor is defined below

$$\tau = \begin{matrix} 2\left(\mu_B + \frac{P_z}{\sqrt{2\pi}}\right)e_{ij},\ \pi > \pi_c \\ 2\left(\mu_B + \frac{P_z}{\sqrt{2\pi}}\right)e_{ij},\ \pi\ < \pi_c \end{matrix} \tag{3}$$

where P_z is the yield stress of the field, π is the product of the component of rate of deformation rate itself, μ_B is a plastic dynamic viscosity of the non-Newtonian fluid, i.e. $\pi = e_{ij}e_{ji}$ and e_{ij} denotes the (i, j) component of the deformation rate and π_c the critical value of π based on non-Newton model.The conservation law of mass, momentum and energy equations takes the following form after applying the boundary layer approximation.

$$\frac{\partial u}{\partial x} + \frac{\partial v}{\partial y} = 0, \tag{4}$$

$$u\frac{\partial u}{\partial x} + v\frac{\partial u}{\partial y} = \frac{\mu}{\rho_0}\left(1+\frac{1}{\beta}\right)\frac{\partial^2 u}{\partial y^2} + v\left(1+\frac{1}{\beta}\right)\frac{\partial u}{\partial y}\frac{\partial \mu}{\partial y} - \frac{\sigma B_0^2}{\rho}u, \tag{5}$$

$$\rho c_p V\cdot\nabla T = -\nabla\cdot q, \tag{6}$$

where u and v are the velocity components along x and y-directions respectively, v is the kinematic viscosity, c_p is the specific heat, ρ is the density, T is the temperature of the fluid, β is the Casson parameter, B_0 is the magnitude of magnetic field, q is the heat flux and μ is the variable viscosity. From Eq. (6)

$$q + \lambda_2\left(\frac{\partial q}{\partial t} + V\cdot\nabla\cdot q - q.\nabla V + (\nabla\cdot V)q\right) = -k\nabla T, \tag{7}$$

where λ_2 is the thermal relaxation time and k is the thermal conductivity of the fluid. Eliminating q from Eqs. (6) and (7) gives:

$$u\frac{\partial T}{\partial x} + v\frac{\partial T}{\partial y} + \lambda_2\left(u\frac{\partial u}{\partial x}\frac{\partial T}{\partial x} + v\frac{\partial v}{\partial y}\frac{\partial T}{\partial y} + u\frac{\partial v}{\partial x}\frac{\partial T}{\partial y} + v\frac{\partial u}{\partial y}\frac{\partial T}{\partial x} + 2uv\frac{\partial^2 T}{\partial x\partial y} + u^2\frac{\partial^2 T}{\partial x^2} + v^2\frac{\partial^2 T}{\partial y^2}\right) = \frac{k}{\rho c_p}\frac{\partial^2 T}{\partial y^2}. \tag{8}$$

The boundary conditions for the present problem are:

$$u = U_w(x) = U_0(x+b)^m,\ v = 0,\ T = T_w \text{ at } y = A(x+b)^{\frac{1-m}{2}}, \tag{9}$$

$$u \to 0,\ T \to T_\infty \text{ as } y \to \infty. \tag{10}$$

Considering the following transformations

$$\eta=\sqrt{\frac{(m+1)U_0(x+b)^{m-1}}{2\nu}}y,\ \psi=\sqrt{\frac{2\nu U_0(x+b)^{m+1}}{m+1}}F(\eta),$$
$$u=U_0(x+b)^m F'(\eta),\ \ v=-\sqrt{\frac{(m+1)\nu U_0(x+b)^{m-1}}{2}}\left[F(\eta)+\eta\frac{m-1}{m+1}F'(\eta)\right],$$
$$\Theta(\eta)=\frac{T-T_\infty}{T_w-T_\infty}. \tag{11}$$

The governing equations are reduced to the following equations:

$$\left(1+\frac{1}{\beta}\right)(1-B\Theta)(F'''-B\Theta'F')+FF'-\frac{2m}{m+1}(F')^2-M^2F'=0, \tag{12}$$

$$\Theta''+\mathrm{Pr}F\Theta'+\mathrm{Pr}\gamma\left(\frac{m-3}{2}FF'\Theta'-\frac{m+1}{2}F^2\Theta''\right)=0, \tag{13}$$

the boundary conditions becomes

$$\begin{aligned} F(\alpha)=&\ \ \frac{\alpha(1-m)}{(1+m)},\ F'(\alpha)=1,\ \Theta(0)=1,\\ F'(\infty)\to&\ \ 0,\ \Theta(\infty)\to 0, \end{aligned} \tag{14}$$

where $\alpha=A\sqrt{\frac{U_0(m+1)}{2\nu}}$ denotes the plat surface. In order to dimensionalize the required equations and boundary conditions define $F(\zeta)=f(\eta-\alpha)=f(\eta)$ which gives

$$\left(1+\frac{1}{\beta}\right)(1-B\theta)(f'''-B\theta'f')+ff'-\frac{2m}{m+1}(f')^2-M^2f'=0, \tag{15}$$

$$\theta''+\mathrm{Pr}f\theta'+\mathrm{Pr}\gamma\left(\frac{m-3}{2}ff'\theta'-\frac{m+1}{2}f^2\theta''\right)=0, \tag{16}$$

$$\begin{aligned} f(0)=&\ \ \frac{\alpha(1-m)}{(1+m)},f'(0)=1,\theta(0)=1,\\ f'(\infty)\to&\ \ 0,\ \theta(\infty)\to 0. \end{aligned} \tag{17}$$

where $M^2=\frac{2\sigma B_0^2}{(m+1)\rho U_0^2(x+b)^{m-1}}$ is Hartmann number, $B=e^{-\zeta(T-T_\infty)}$ is the variable viscosity parameters, $\mathrm{Pr}=\frac{\mu c_p}{k}$ is Prandtl number and $\gamma=\lambda_2U_0(x+b)^{m-1}$ is the thermal relaxation parameters.

The wall shear stress at the sheet is given by

$$\tau_w=\mu\left(1+\frac{1}{\beta}\right)\frac{\partial u}{\partial y}, \tag{18}$$

the skin friction can be defined as

$$C_f=\frac{\tau_w}{\sqrt{(m+1)U_0}2\nu}\left(\frac{1}{(x+b)^{\frac{3m-1}{2}}}\right), \tag{19}$$

while the dimensionless forms of skin friction

$$C_f\sqrt{Re_x}=\left[\left(1+\frac{1}{\beta}\right)(1-B\theta)f'\right]_{\eta=0}, \tag{20}$$

Where $\mathrm{Re}_x=\sqrt{\frac{U_0}{\nu}}x$.

3. Numerical solutions

The numerical solutions of non-linear ordinary differential Eqs. (15) and (16) subject to boundary condition Eq. (17) are obtained by Keller box method. Let $u(x,\eta)$, $u(x,\eta)$, $p(x,\eta)$ and $q(x,\eta)$ with $u=f$, $v=u'$, $q=\theta'$ and $p=q'$, Eqs. (15) and (16) reduces to first order form, i.e.

$$\left(1+\frac{1}{\beta}\right)(1-B\theta)(v'-Bq'v)+fv-\frac{2m}{m+1}u^2-M^2u=0, \tag{21}$$

$$q'+\mathrm{Pr}^qf+\mathrm{Pr}^\gamma\left(\frac{m-3}{2}fuq-\frac{m+1}{2}f^2q'\right)=0. \tag{22}$$

The rectangular grid in x–η plane is shown in Fig. 2 and the net points are:

$$\begin{aligned} x^0=&\ \ 0,x^i=x^{i-1}+k_i,i=1,\ 2,\ 3,\ldots I,\\ \eta_0=&\ \ 0,\eta_j=\eta_{j-1}+h_j,j=1,\ 2,\ 3,\ldots J, \end{aligned}$$

where k_i and h_j are the Δx and $\Delta\eta$ -spacing.

Using central difference formulation at midpoint $(x^i,\eta_{j-1/2})$ as

$$[f_j^i-f_{j-1}^i]=\frac{h_j}{2}[u_j^i+u_{j-1}^i], \tag{23}$$

$$\frac{u_j^i-u_{j-1}^i}{h_j}=\frac{v_j^i+v_{j-1}^i}{2}, \tag{24}$$

$$\frac{p_j^i-p_{j-1}^i}{h_j}=\frac{q_j^i+q_{j-1}^i}{2}. \tag{25}$$

Similarly at point $(x^{i-1/2},\eta_{j-1/2})$, Eqs. (21) and (22) gives

$$\begin{aligned} &\left(1+\frac{1}{\beta}\right)(1-B\theta)\left(v_j^i-v_{j-1}^i-hB\left(q_{j-\frac{1}{2}}^iv_{j-1/2}^i\right)\right)+hf_{j-1/2}^iv_{j-1/2}^i\\ &-h\left(\frac{2m}{m+1}\right)\left(u_{j-1/2}^i\right)^2-hM^2u_{j-1/2}^i=R_{j-1/2}, \end{aligned} \tag{26}$$

$$\begin{aligned} &(q_j^i-q_{j-1}^i)+\mathrm{Pr}^hq_{j-1/2}^if_{j-1/2}^i+\mathrm{Pr}h\gamma\left(\frac{m-3}{2}\right)q_{j-1/2}^iu_{j-1/2}^if_{j-1/2}^i\\ &-\mathrm{Pr}\gamma\left(\frac{m+1}{2}\right)\left(f_{j-1/2}^i\right)^2\left(q_j^i-q_{j-1}^i\right)=T_{j-1/2}, \end{aligned} \tag{27}$$

where

$$\begin{aligned} R_{j-1/2}=&-\left(1+\frac{1}{\beta}\right)(1-B\theta)\left(\left(v_j^{i-1}-v_{j-1}^{i-1}-hB\left(q_{j-\frac{1}{2}}^iv_{j-1/2}^i\right)\right)\right.\\ &\left.+hf_{j-1/2}^{i-1}v_{j-1/2}^{i-1}-h\left(\frac{2m}{m+1}\right)\left(u_{j-1/2}^{i-1}\right)^2-hM^2u_{j-1/2}^{i-1}\right), \end{aligned} \tag{28}$$

and

$$\begin{aligned} T_{j-1/2}=&-((q_j^{i-1}-q_{j-1}^{i-1})+\mathrm{Pr}hq_{j-1/2}^{i-1}f_{j-1/2}^{i-1}\\ &+\mathrm{Pr}h\gamma\left(\frac{m-3}{2}\right)q_{j-1/2}^{i-1}u_{j-1/2}^{i-1}f_{j-1/2}^{i-1}\\ &-\mathrm{Pr}\gamma\left(\frac{m+1}{2}\right)\left(f_{j-1/2}^{i-1}\right)^2(q_j^{i-1}-q_{j-1}^{i-1})), \end{aligned} \tag{29}$$

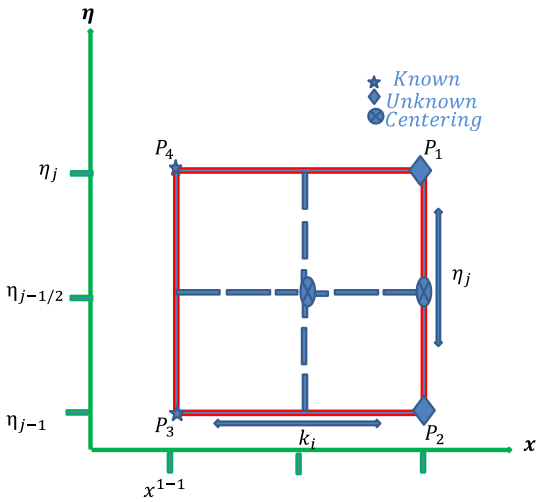

Fig. 2. Schematic representation of domain.

such that $R_{j-1/2}$ and $T_{j-1/2}$ are known quantities.

The following boundary conditions reduces to

$$f_0^i = \frac{\alpha(1-m)}{(1+m)},\ u_0^i = 1,\ u_j^i = 0,\ p_0^i = 1,\ p_j^i = 0. \tag{30}$$

Newton's method is used to linearize Eqs. (22)–(26).

For this case

$$f_j^{(i+1)} = f_j^{(i)} + \delta f_j^{(i)},\ u_j^{(i+1)} = u_j^{(i)} + \delta u_j^{(i)},\ v_j^{(i+1)} = v_j^{(i)} + \delta v_j^{(i)},$$
$$p_j^{(i+1)} = p_j^{(i)} + \delta p_j^{(i)},\ q_j^{(i+1)} = q_j^{(i)} + \delta q_j^{(i)}, \tag{31}$$

put Eq. (31) in Eqs. (26) and (27) and neglecting higher order of δ

$$\delta f_j - \delta f_{j-1} - \frac{h_j}{2}(\delta u_j + \delta u_{j-1}) = (r_1)_j, \tag{32}$$

$$\delta u_j - \delta u_{j-1} - \frac{h_j}{2}(\delta v_j + \delta v_{j-1}) = (r_2)_j, \tag{33}$$

$$\delta p_j - \delta p_{j-1} - \frac{h_j}{2}(\delta q_j + \delta q_{j-1}) = (r_3)_j, \tag{34}$$

$$(a_1)_{j-1/2}\delta v_j + (a_2)_{j-1/2}\delta v_{j-1} + (a_3)_{j-1/2}\delta u_j + (a_4)_{j-1/2}\delta u_{j-1} + (a_5)_{j-1/2}\delta f_j$$
$$+(a_6)_{j-1/2}\delta f_{j-1} = (r_4)_{j-1/2}, \tag{35}$$

$$(b_1)_{j-1/2}\delta q_j + (b_2)_{j-1/2}\delta q_{j-1} + (b_3)_{j-1/2}\delta u_j + (b_4)_{j-1/2}\delta u_{j-1} + (b_5)_{j-1/2}\delta f_j$$
$$+(b_6)_{j-1/2}\delta f_{j-1} = (r_5)_{j-1/2}, \tag{36}$$

where

$$(a_1)_{j-1/2} = \left(1+\frac{1}{\beta}\right)(1-B\theta) + \frac{hf_{j-1/2}}{2} - \frac{Bh}{2}q^i_{j-1/2}, \tag{37}$$

$$(a_2)_{j-1/2} = -\left(1+\frac{1}{\beta}\right)(1-B\theta) + \frac{hf_{j-1/2}}{2} - \frac{Bh}{2}q^i_{j-1/2}, \tag{38}$$

$$(a_3)_{j-1/2} = -\left(\frac{mh}{m+1}\right)u_{j-1/2} - \frac{hM^2}{2},\ (a_4)_{j-1/2} = (a_3)_{j-1/2}, \tag{39}$$

$$(a_5)_{j-1/2} = \frac{hv_{j-1/2}}{2},\ (a_5)_{j-1/2} = (a_5)_{j-1/2}, \tag{40}$$

$$(a_6)_{j-1/2} = \frac{hv_{j-1/2}q^i_{j-1/2}}{2},\ (a_7)_{j-1/2} = (a_6)_{j-1/2}, \tag{41}$$

$$(b_1)_{j-1/2} = 1 + \frac{\mathrm{Pr}hf_{j-1/2}}{2} + \mathrm{Pr}h\gamma\left(\frac{m-3}{4}\right)f_{j-1/2}u_{j-1/2}$$
$$-\mathrm{Pr}gamma\left(\frac{m+1}{2}\right)f^2_{j-1/2}, \tag{42}$$

$$(b_2)_{j-1/2} = -1 + \frac{\mathrm{Pr}hf_{j-1/2}}{2} + \mathrm{Pr}h\gamma\left(\frac{m-3}{4}\right)f_{j-1/2}u_{j-1/2}$$
$$-\mathrm{Pr}\gamma\left(\frac{m+1}{2}\right)f^2_{j-1/2}, \tag{43}$$

$$(b_3)_{j-1/2} = \frac{f_{j-1/2}q_{j-1/2}}{2}, \tag{44}$$

$$(b_4)_{j-1/2} = (b_3)_{j-1/2}, \tag{45}$$

$$(b_5)_{j-1/2} = \frac{\mathrm{Pr}hq_{j-1/2}}{2} + \mathrm{Pr}h\gamma\left(\frac{m-3}{4}\right)q_{j-1/2}u_{j-1/2}$$
$$-\mathrm{Pr}\gamma h\left(\frac{m+1}{2}\right)f_{j-1/2}q'_{j-1/2}, \tag{46}$$

$$(b_6)_{j-1/2} = (b_5)_{j-1/2}, \tag{47}$$

$$(r_4)_{j-1/2} = -hf_{j-1/2}v_{j-1/2} + \frac{2m}{m+1}h(u_{j-1/2})^2 + hM^2u_{j-1/2} + R_{j-1/2}, \tag{48}$$

$$(r_5)_{j-1/2} = -(q_j - q_{j-1}) - \mathrm{Pr}hq_{j-1/2}f_{j-1/2}$$
$$-\mathrm{Pr}\gamma h\left(\frac{m+1}{2}\right)f^2_{j-1/2}q'_{j-1/2} + T_{j-1/2}, \tag{49}$$

the boundary conditions become

$$\delta f_0 = 0,\ \delta u_0 = 0,\ \delta p_0 = 0,\ \delta u_J = 0,\ \delta p_J = 0. \tag{50}$$

Writing Eqs. (33)–(37) in block tridiagonal matrix form. i.e.

$$\begin{bmatrix} [A_1] & [C_1] & & & \\ [B_1] & [A_2] & [C_2] & & \\ & - & - & & \\ & & [B_{J-1}] & [A_{J-1}] & [C_{J-1}] \\ & & & [B_J] & [A_J] \end{bmatrix} \begin{bmatrix} [\delta_1] \\ [\delta 2] \\ - \\ [\delta_{J-1}] \\ [\delta_J] \end{bmatrix} = \begin{bmatrix} [r_1] \\ [r_2] \\ - \\ [r_{J-1}] \\ [r_J] \end{bmatrix}$$

that is:

$$[A][\delta] = [r], \tag{51}$$

where the elements are

$$[A_1] = \begin{bmatrix} 0 & 0 & 1 & 0 & 0 \\ -\frac{h_1}{2} & 0 & 0 & -\frac{h_1}{2} & 0 \\ 0 & -\frac{h_1}{2} & 0 & 0 & -\frac{h_1}{2} \\ (a_2)_1 & (a_8)_1 & (a_5)_1 & (a_1)_1 & (a_7)_1 \\ 0 & (b_2)_1 & (b_5)_1 & 0 & (b_1)_1 \end{bmatrix}, \tag{52}$$

$$[A_J] = \begin{bmatrix} 0 & 0 & -1 & 0 & 0 \\ -1 & 0 & 0 & -\frac{h_j}{2} & 0 \\ 0 & 0 & 0 & 0 & -\frac{h_j}{2} \\ 0 & 0 & (a_6)_j & (a_2)_j & (a_8)_1 \\ 0 & 0 & (b_6)_j & 0 & (b_2)_j \end{bmatrix}, 2 \leqslant j \leqslant J \tag{53}$$

$$[B_J] = \begin{bmatrix} -\frac{h_j}{2} & 0 & 1 & 0 & 0 \\ -1 & 0 & 0 & -\frac{h_j}{2} & 0 \\ 0 & -1 & 0 & 0 & -\frac{h_j}{2} \\ (a_4)_j & 0 & (a_5)_j & (a_1)_j & (a_7)_j \\ (a_4)_j & 0 & (b_5)_j & 0 & (b_1)_j \end{bmatrix}, 2 \leqslant j \leqslant J \tag{54}$$

$$[C_J] = \begin{bmatrix} -\frac{h_j}{2} & 0 & 0 & 0 & 0 \\ 1 & 0 & 0 & 0 & 0 \\ 0 & 1 & 0 & 0 & 0 \\ (a_3)_j & 0 & 0 & 0 & 0 \\ (b_3)_j & 0 & 0 & 0 & 0 \end{bmatrix}, 2 \leqslant j \leqslant J \tag{55}$$

to solve Eq. (51), assume that A is nonsingular and can be factored into

$$[A] = [LIU] \tag{56}$$

where

$$[L] = \begin{bmatrix} [\alpha_1] & & & & \\ [B_2] & [\alpha_2] & & & \\ & - & - & & \\ & & - & [\alpha_{J-1}] & \\ & & & [B_J] & [\alpha_J] \end{bmatrix}$$

and

$$[U] = \begin{bmatrix} [I] & [T_1] & & & \\ & [I] & [T_2] & & \\ & & - & & \\ & & & [I] & [T_{J-1}] \\ & & & & [I] \end{bmatrix},$$

where [I] is the identity matrix of order 5 and $[\alpha_i]$, and $[T_i]$ are 5×5 matrices which elements are determent by the following equation:

$$[\alpha_1] = [T_1], \tag{57}$$

$$[\alpha_1][T_1] = [C_1], \tag{58}$$

and

$$[\alpha_j] = [A_j] - [B_j][T_{j-1}], \tag{59}$$

$$[\alpha_j][T_j] = [C_j], \tag{60}$$

Eq. (56) can now be substituted into Eq. (51), we get

$$[LIUI\delta] = [r], \tag{61}$$

If we define

$$[UI\delta] = [W], \tag{62}$$

then Eq. (61) becomes

$$[LIW] = [r], \tag{63}$$

where

$$W = \begin{bmatrix} W_1 \\ W_2 \\ \\ W_{J-1} \\ W_J \end{bmatrix},$$

where $[W_j]$ are 5×1 column matrices. The elements w can be solved from Eq. (63)

$$[\alpha_1][w_1] = [r_1], \tag{64}$$

$$[\alpha_j][W_j] = [r_j] - [B_j][W_{j-1}], \tag{65}$$

The step in which T, α and W_j are calculated is usually referred to as the forward sweep. Once the elements of W are found, Eq. (62) gives the solution so-called backward sweep, in which the elements are obtained by following relations:

$$[\delta_j] = [W_j], \tag{66}$$

$$[\delta_j] = [W_j] - [T_j][\delta_{j+1}],\ 1 \leqslant j \leqslant J-1. \tag{67}$$

Once the elements of are found, Eq. (37) can be used to find the $(i+1)$-th iteration in Eq. (31). These calculation are repeated until some convergence criterion is satisfied and calculations are stopped when

$$\delta v_0^{(i)} \leqslant x, \tag{68}$$

where $x = 0.001$ is a small value.

4. Discussion

In this section, the influence of various pertinent parameters such as Casson fluid parameter β, variable viscosity parameter B, Hartmann number M, thermal relaxation parameter γ and Prandtl number Pr are deliberated for velocity and temperature profiles. Fig. 3 shows the effect of the Casson fluid parameter v on velocity profile. It is observed that the Casson parameter β creates a resistive-type force in the fluid flow. Consequently, the magnitude of the velocity profile and boundary layer thickness reduces for higher values of β. It is clear from Fig. 4 that temperature profile reduces for higher value of Prandtl number Pr . The Prandtl number Pr is contrariwise connected with thermal diffusivity. An increase in Prandtl number Pr corresponds to decrease the thermal diffusivity, which causes temperature of the fluid to reduce. From Fig. 5 it is observed that for higher value of Hartmann number M, magnitude of velocity profile and boundary layer thickness reduces. Because an increase in magnetic field up rises the opposite force to the flow direction, which is called resistive-type force (Lorentz force), which redueces the velocity profile. Fig. 6 shows the impact of wall thickness parameter α on velocity profile. It is evaluated that the boundary layer thickness and the velocity profile reduces with the increase in wall thickness parameter α. Because by increasing wall thickness parameter α, stretching velocity of the plate reduces which results reduction in the velocity profile Fig. 7 describes the influence of power index m on velocity profile. On increasing the power index m the stretching velocity increases which produce distortion in the fluid causing velocity of the fluid to increase. Fig. 8 shows the impact of thermal relaxation parameter γ on temperature profile. It is clear that temperature distribution and thermal boundary layer thickness reduces for higher values of wall thickness parameter γ.

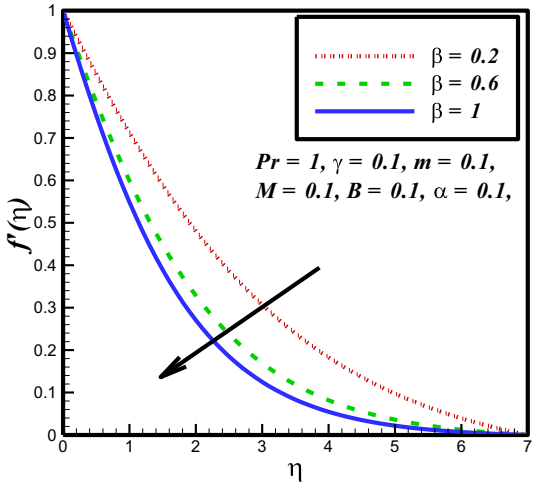

Fig. 3. Influence of β on $f'(\eta)$.

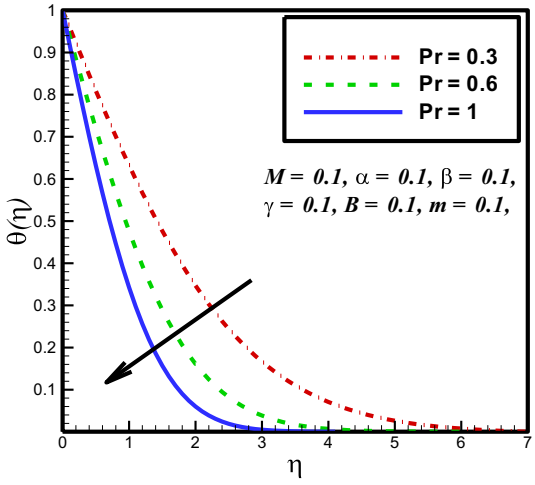

Fig. 4. Influence of Pr on $\theta(\eta)$.

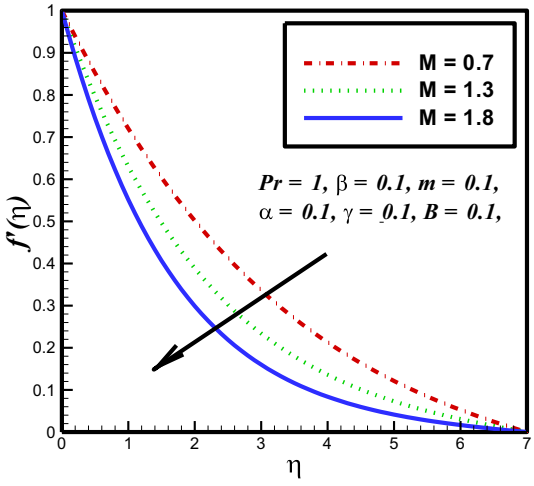

Fig. 5. Influence of M on $f'(\eta)$.

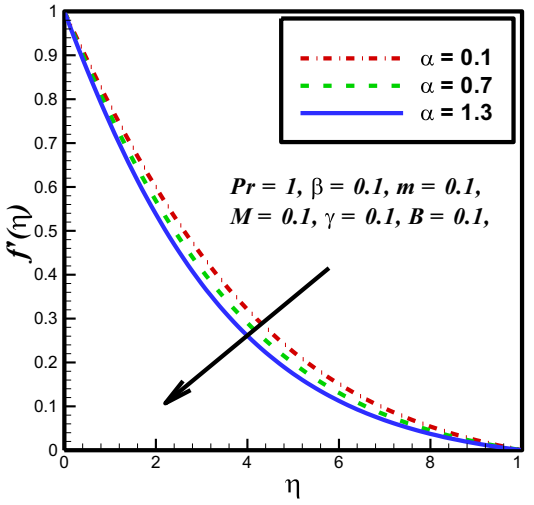

Fig. 6. Influence of α on $f'(\eta)$.

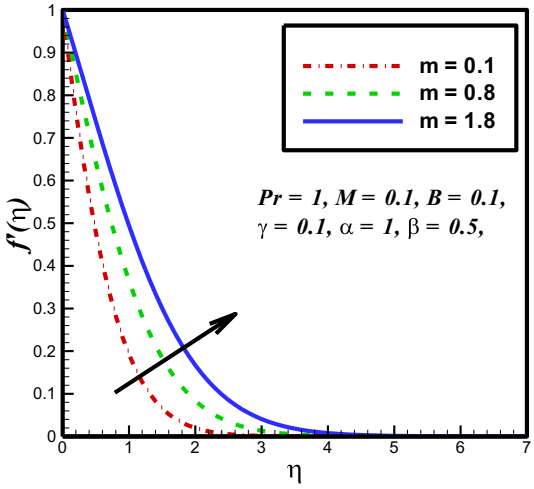

Fig. 7. Influence of m on $f'(\eta)$.

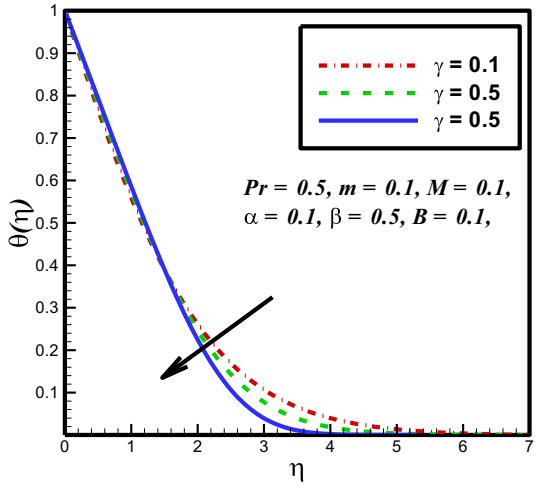

Fig. 8. Influence of γ on $\theta(\eta)$.

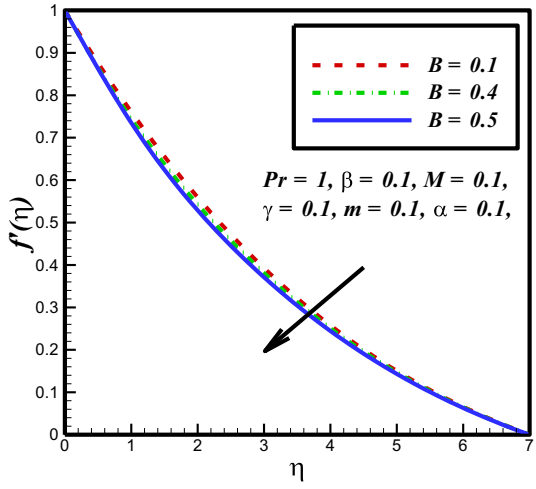

Fig. 9. Influence of B on $f'(\eta)$.

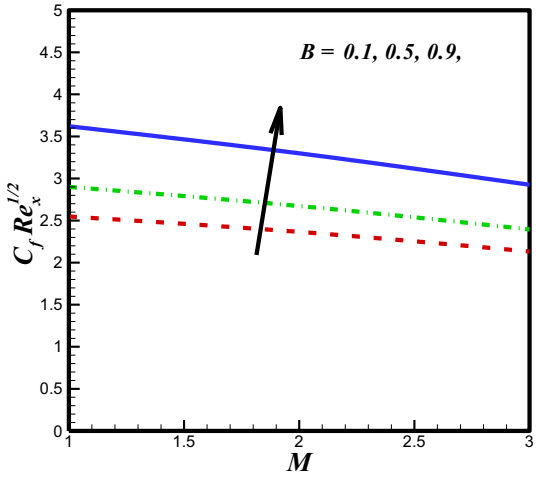

Fig. 10. Influence of B and M on skin friction coefficient.

Physically, an increase in thermal relaxation parameter causes less transfer of heat from sheet to the fluid. So temperature of the fluid reduces with the increase in thermal relaxation parameter. Fig. 9 shows the physical behavior of variable viscosity parameter B on velocity profile. It is obvious from the figure that velocity of the fluid reduces with the increase in variable viscosity parameter B. This is because as the variable viscosity parameter B is increased the thickness of the fluid particles increases which

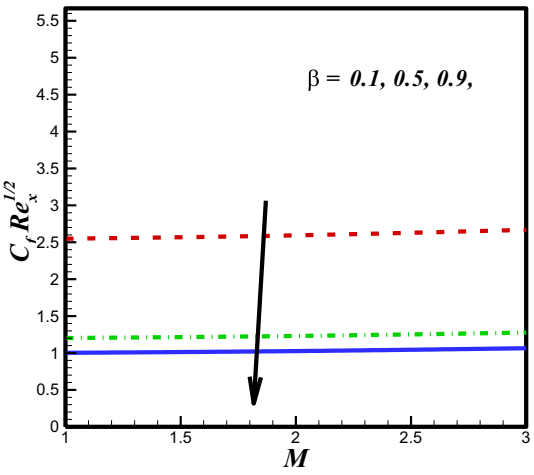

Fig. 11. Influence of β and M on skin friction coefficient.

Table 1
Comparison of the present results for $f''(0)$ with the literature on varying Hartmann number M when Pr = 1 , $\gamma = \beta = \alpha = 0$ but $m = 1$.

M	Akbar et al. [30]	Salahuddin et al. [31]	Present Results
0	1	1	1
0.5	−1.11803	−1.11801	−1.118105
1	−1.41421	−1.41418	−1.14415
5	−2.44949	−2.44942	−2.44947
10	−3.31663	−3.31656	−3.31696
100	−10.04988	−10.04981	−10.04983
500	−22.38303	−22038293	−22.38284
1000	−31.63839	−31.63846	−31.63851

Table 2
Comparison of $-\theta'(0)$ for different values of Prandtle number Pr when $\gamma = M = \alpha = \beta = 0$ but $m = 1$.

Pr	Wang [32]	Salahuddin et al. [31]	Present result
0.07	0.0656	0.0654	0.0651
0.20	0.1691	0.1688	0.1683
0.70	0.4539	0.4534	0.4537
2.00	0.9114	0.9108	0.9109
7.00	1.8954	1.8944	1.8948
20.00	3.3539	3.3522	3.3521
70.00	6.4622	6.4619	6.4626

Table 3
Numerical effects the skin friction coefficient for the different values B, β and M.

M	B	β	$-C_f Re_x^{1/2}$
0.1	0.1	0.1	2.5862
0.2	0.1	0.1	2.6353
0.3	0.1	0.1	2.7160
0.1	0.1	0.1	2.5862
0.1	0.2	0.1	2.3154
0.1	0.1	0.1	2.0423
0.1	0.1	0.1	2.5862
0.1	0.1	0.2	1.8849
0.1	0.1	0.3	1.6303

disrespects the velocity of the fluid to decrease. Figs. 10 and 11, present the influence of Hartmann number M on local skin friction coefficient for different values of variable viscosity parameter B and Casson fluid parameter β. It is cleared from Fig. 10 that for large values of Hartmann number M and variable viscosity parameter B the skin friction coefficient increases. Whereas, Fig. 11 shows that skin friction coefficient reduces for large values of Casson fluid parameter β. Table 1 and 2 shows the comparison of the present work with the previous literature. It is observed that the obtained results are in excellent agreement with the published work [30–32]. Table 3 shows the effect of different physical parameters on skin friction coefficient.

5. Conclusions

An analysis is done to solve the MHD flow of Casson fluid model over a stretching sheet with variable thickness by assuming the viscosity of the fluid to be variable. Cattaneo-Chirstov heat flux model is used to discover the heat relocation phenomena. Keller box method is applied to solve the governing nonlinear differential equations. The main findings of this problem are listed below.

Velocity reduces for the large values of wall thickness parameter α.

- For large values of power index m the velocity profile increases.
- Temperature profile increases more rapidly in Fourier's law case instead of Cattaneo–Christov heat flux model.
- Velocity profile reduces for higher values of Hartmann number M and variable viscosity B.

The momentum boundary layer thickness decreases for large values of Casson fluid parameter β.

References

[1] S. Nadeem, R.U. Haq, C. Lee, MHD flow of a Casson fluid over an exponentially shrinking sheet, Sci. Iran. 19 (2012) 1550–1553.
[2] S. Mukhopadhyay, P.R. De, K. Bhattacharyya, G.C. Layek, Casson fluid flow over an unsteady stretching surface, Ain Shams Eng. J. 4 (2013) 933–938.
[3] S. Mukopadhyay, Casson fluid flow and heat transfer over a nonlinearly stretching surface, Chin. Phys. 22 (2013) 074701.
[4] S. Nadeem, R.U. Haq, N.S. Akbar, Z.H. Khan, MHD three-dimensional Casson fluid flow past a porous linearly stretching sheet, Alexandria Eng. J. 52 (2013) 577–582.
[5] S. Mukhopadhyaya, I.C. Moindala, T. Hayat, MHD boundary layer flow of Casson fluid passing through an exponentially stretching permeable surface with thermal radiation, Chin. Phys. 23 (2014) 104701.
[6] G. Mahanta, S. Shaw, 3D Casson fluid flow past a porous linearly stretching sheet with convective boundary condition, Alexandria Eng. J., http://dx.doi.org/10.1016/j.aej.2015.04.014.
[7] M. Mustafa, J.A. Khan, Model for flow of Casson nanofluid past a non-linearly stretching sheet considering magnetic field effects, AIP Adv. 5 (2015) 077148.
[8] I.L. Animasaun, E.A. Adebile, A.I. Fagbade, Casson fluid flow with variable thermo-physical property along Exponentially stretching sheet with suction and exponentially decaying internal heat generation using the homotopic analysis Method, J. Niger. Math. Soc. (2015), http://dx.doi.org/10.1016/j.jnnms.2015.02.001.
[9] M. Das, R. Mahato, R. Nandkeolyar, Newtonian heating effect on unsteady hydro-magnetic Casson fluid flow past a flat plate with heat and mass transfer, Alexandria Eng. J. (2015), http://dx.doi/10.1016/j.aej.2015.07.007.
[10] C.S.K. Raju, N. Sandeep, V. Sugunamma, M.J. Babu, J.V.R. Reddy, Heat and mass transfer in magnetohydrodynamic Casson fluid over an exponentially permeable stretching surface, Eng. Sci. Technol. Int. J. 19 (1) (2016) 45–52.
[11] K. Ramesh, M. Devakar, Some analytical solutions for flows of Casson fluid with slip boundary conditions, Ain Shams Eng. J. 6 (2015) 967–975.
[12] A. Khalid, I. Khan, A. Khan, S. Shafie, Unsteady MHD free convection flow of Casson fluid past over an oscillating vertical plate embedded in a porous medium, Eng. Sci. Technol. Int. J. 18 (3) (2015) 309–317.
[13] N.V. Ganesh, B. Ganga, A.K.A. Hakeem, Lie symmetry group analysis of magnetic field effects on free convective flow of a nano fluid over a semi-infinite stretching sheet, J. Egypt. Math. Soc. 22 (2014) 304–310.
[14] H. Dessie, N. Kishan, MHD effects on heat transfer over stretching sheet embedded in porous medium with variable viscosity, viscous dissipation and heat source/sink, Ain Shams Eng. J. 5 (2014) 967–977.
[15] A.K.A. Hakeem, R. Kalaivanan, N.V. Ganesh, B. Ganga, Effect of partial slip on hydro magnetic flow over a porous stretching sheet with non-uniform heat source/sink, thermal radiation and wall mass transfer, Ain Shams Eng. J. 5 (2014) 913–922.
[16] R.D. Ene, V. Marinca, Approximate solutions for steady boundary layer MHD viscous flow and radiative heat transfer over an exponentially porous stretching sheet, Appl. Math. Comput. 269 (2015) 389–401.
[17] Z. Abbas, S. Rasool, M.M. Rashidi, Heat transfer analysis due to an unsteady stretching/shrinking cylinder with partial slip condition and suction, Ain Shams Eng. J. 6 (2015) 939–945.

[18] T. Hayat, M.S. Anwar, M. Farooq, A. Alsaedi, Mixed convection flow of viscoelastic fluid by a stretching cylinder with heat transfer, PLoS One (2015), http://dx.doi.org/10.1371/journal.pone.0118815.
[19] M.Y. Malik, T. Salahuddin, A. Hussain, S. Bilal, MHD flow of tangent hyperbolic fluid over a stretching cylinder: using Keller box method, J. Magn. Magn. Mater. 395 (2015) 271–276.
[20] N. Sandeep, C. Sulochana, B. Rushi Kumar, Unsteady MHD radiative flow and heat transfer of a dusty nano fluid over an exponentially stretching surface, Eng. Sci. Technol. Int. J. 19 (1) (2016) 227–240.
[21] T. Fang, J. Zhang, Y. Zhong, Boundary layer flow over a stretching sheet with variable thickness, Appl. Math. Comput. 218 (2012) 7241–7252.
[22] M.M. Khader, A.M. Megahed, Numerical solution for boundary layer flow due to a nonlinearly stretching sheet with variable thickness and slip velocity, Eur. Phys. J. Plus 128 (2013) 100.
[23] G.C. Sarangi, S.K. Mishra, Boundary layer flow and heat transfer of dusty fluid over a stretching sheet, Eng. Sci. Technol. Int. J. 5 (2015) 2250–3498.
[24] M.M. Khader, A.M. Megahed, Boundary layer flow due to a stretching sheet with a variable thickness and slip velocity, J. Appl. Mech. Tech. Phys. (2015), http://dx.doi.org/10.1134/S0021894415020091.
[25] T. Hayat, M. Farooq, A. Alsaedi, F.A. Solamy, Impact of Cattaneo–Christov heat flux in the flow over a stretching sheet with variable thickness, AIP Adv. 5 (2015) 087159.
[26] C.I. Christov, On frame indifferent formulation of the Maxwell-Cattaneo model of finite-speed heat conduction, Mech. Res. Commun. 36 (2009) 481–486.
[27] S. Han, L. Zheng, C. Li, X. Zhang, Coupled flow and heat transfer in viscoelastic fluid with Cattaneo–Christov heat flux model, Appl. Math. Lett. 38 (2014) 87–93.
[28] C.S.K. Raju, N. Sandeep, V. Sugunamma, M.J. Babu, J.V.R. Reddy, Heat and mass transfer in magnetohydrodynamic Casson fluid over an exponentially permeable stretching surface, Eng. Sci. Technol. Int. J. 19 (2016) 45–52.
[29] M. Mustafa, Cattaneo–Christov heat flux model for rotating flow and heat transfer of upper-convicted Maxwell fluid, AIP Adv. 5 (2015) 047109.
[30] N.S. Akbar, A. Ebaud, Z.H. Khan, Numerical analysis of magnetic field effects on Eyring-Powell fluid flow towards a stretching sheet, J. Magn. Magn. Mater. 382 (2015) 355–358.
[31] T. Salahuddin, M.Y. Malik, A. Hussain, S. Bilal, M. Awais, MHD flow of Cattaneo–Christov heat flux model for Williamson fluid over a stretching sheet with variable thickness: using numerical approach, J. Magn. Magn. Mater. 401 (2016) 991–997.
[32] C.Y. Wang, Free convection on a vertical stretching surface with suction and blowing, Appl. Math. Mech. 69 (1989) 418–420.